PHYSICAL REVIEW D **87,** 013007 (2013)

Dipole-interacting fermionic dark matter in positron, antiproton, and gamma-ray channels

Jae Ho Heo* and C. S. Kim†

Department of Physics and IPAP, Yonsei University, Seoul 120-479, Korea

(Received 16 October 2012; published 18 January 2013)

Cosmic ray signals from dipole-interacting dark matter annihilation are considered in the positron, antiproton, and photon channels. The predicted signals in the positron channel could nicely account for the excess of positron fraction from Fermi LAT, PAMELA, HEAT, and AMS-01 experiments for the dark matter mass larger than 100 GeV with a boost (enhancement) factor of 30–80. No excess of antiproton over proton ratio at the experiments also gives a severe restriction for this scenario. With the boost factors, the predicted signals from Galactic halo and signals as monoenergetic gamma-ray lines (monochromatic photons) for the region close to the Galactic center are investigated. The gamma-ray excess of recent tentative analyses based on Fermi LAT data and the potential probe of the monochromatic lines at a planned experiment, AMS-02, are also considered.

DOI: 10.1103/PhysRevD.87.013007 PACS numbers: 13.40.Em, 14.80.−j, 95.35.+d, 98.70.Sa

I. INTRODUCTION

The existence of dark matter (DM), as the invisible matter interacting by the force of gravity, has been widely accepted by cosmological observations from the experiments such as Cosmic Microwave Background (CMB) [1], Galactic Rotation Curves [2], Gravitational Lensing [3], and Massive Compact Halo Objects [4]. About 83% of the matter (around 23% of the total energy density) in the Universe is believed to be composed of DM to account for the observations. However, the nature of DM is still completely unknown despite decades of detection efforts. Many possible explanations have been proposed. One of the alternative explanations from the point of view of particle physics is that DM is composed of massive particles and its interaction with ordinary matter is very weak.

Recently several DM models[1] (inelastic DM [7,8], asymmetric DM [9], form factor DM [10]) with magnetic dipole interaction have been considered. DM in these models has a few states and has no direct interaction with the photon. The candidate particles could thus be stable and make up the invisible matter in our Universe. On the other hand, the direct interaction with a photon through magnetic dipole coupling has gotten some attention [11–17] due to its plausibility. Most of the works have concentrated on direct detections of DM. The main motivation for the magnetic dipole interacting DM scenario is that the magnetic dipole coupling can be sizable compared to other electromagnetic couplings, because the magnetic dipole conserves the discrete symmetries like parity (P), time reversal (T), and charge conjugation (C) or combinations of the same.

In this work, we consider cosmic ray signatures (indirect detections) of the direct dipole-interacting DM with the shifted photon (hypercharge gauge boson B_μ). The cosmic ray signatures in the positron, antiproton, and photon channels are considered for the DM mass near the electroweak scale (10–1000 GeV), essentially around 100 GeV. The dimension-five operator that induces the dipole interaction is $\bar{\psi}\sigma_{\mu\nu}\psi B^{\mu\nu}$, and it may be expressed with a photon and a Z boson in the standard model context since the hypercharge gauge boson is a linear combination of a photon and a Z boson with Weinberg angle θ_W. The relevant effective Lagrangian is given by

$$\mathcal{L}_{\text{eff}} = \frac{1}{2}\mu\bar{\psi}\sigma_{\mu\nu}\psi(F^{\mu\nu} - \tan\theta_W Z^{\mu\nu}), \qquad (1)$$

where $F^{\mu\nu}$ is the field strength for the photon, $Z^{\mu\nu}$ is for the Z boson, and μ is the magnetic dipole moment. The DM annihilations therefore produce the standard model particles via γ, Z exchanges. The annihilation processes were studied in Ref. [11] in detail, and here we take advantage of the results (annihilation rates or fractions). The corresponding annihilation fractions are tabulated in Table I for our benchmark mass, 100 GeV.

II. COSMIC RAY SIGNATURES

DM may annihilate at some point in the Galaxy and produce the standard model particles. These produced particles then propagate in the interstellar medium. Antimatter particles and photons have been considered to be the subject of indirect DM searches, because antimatter particles are rarely produced in astrophysical process and gamma rays can transport freely without energy loss or transmutation of the direction. They may thus provide

*jaeheo1@gmail.com
†Corresponding author.
cskim@yonsei.ac.kr

[1]Actually these models have been built to explain the annual modulation signal from DAMA/NaI [5] and DAMA/LIBRA [6] experiments with null results from other experiments (there is no experimental evidence corroborating this signal yet). The scenario in Ref. [7] is especially interesting, because the signal appears to be an electromagnetic energy deposit, not nuclear energy deposit, through the single photon emission by the decay of the excited state.

TABLE I. Annihilation fractions for each channel, in which u denotes up type quarks ($= u, c$), d down type quarks ($= d, s, b$), ν neutrinos ($= \nu_e, \nu_\mu, \nu_\tau$), and e charged leptons ($= e, \mu, \tau$). Five fundamental channels are considered for dark matter mass of 100 GeV.

Channel	$u\bar{u}$	$d\bar{d}$	$\nu\bar{\nu}$	$e\bar{e}$	W^+W^-
Annihilation fraction (%)	14.6	7.4	3.2	10.1	8.3

important signatures of DM in the Galaxy. Observations of such signals can reveal information on the microscopic nature of DM.

The emissivity/energy (production rate or source for the signals)[2] at location $\mathbf{x}$ from the Galactic center is obtained from the convolution over the various annihilation channels f of the annihilation rate $\langle\sigma v\rangle_f$ with the differential yield (single particle spectra)[3] $(dN^f/dT)_a$ for the final state particles a,

$$Q_a(\mathbf{x}, T) = \frac{1}{4} B\langle\sigma v\rangle_f \left(\frac{dN^f}{dT}\right)_a \left(\frac{\rho(\mathbf{x})}{M}\right)^2, \tag{2}$$

where M is the DM mass, B is an overall boost (enhancement) factor, and $\rho(\mathbf{x})$ is the DM mass density at the location $\mathbf{x}$. The DM mass density around the Galactic center (DM halo profile) is not known, especially near the center (≤ 100 pc). The theoretically motivated ones are Navarro-Frenk-White (NFW) [23], Moore [24], cored isothermal [25], and recently Einasto profiles [26,27]. The kinetic energy T is often approximated to the total energy E, in the case when the particles are energetic. Notice that the factor $\frac{1}{4}$ is different from the one of self-annihilating DM.

The DM density profile can be parametrized as

$$\rho(r) = \rho_\odot \left[\frac{r_\odot}{r}\right]^\gamma \left[\frac{1 + (r_\odot/r_s)^\alpha}{1 + (r/r_s)^\alpha}\right]^{(\beta-\gamma)/\alpha}, \tag{3}$$

where $\rho_\odot \simeq 0.4$ GeV/cm^3 [28] is the DM density in the solar vicinity and $r_\odot = 8.33$ kpc is the distance of the solar system from the Galactic center. The profile parameters α, β, γ, r_s are summarized in Table II. The Einasto profile is $\rho_{\rm Einasto}(r) = \rho_\odot \exp[-(2/\alpha)[(r/r_s)^\alpha - 1)]]$ with $r_s = 20$ kpc and $\alpha = 0.17$. As is well known, the NFW and Moore profiles exhibit a cusp at the center of Galaxy.

[2]If DM is produced with a primordial asymmetry like baryons, there would be almost no signals from DM-anti-DM annihilations due to lack of antidark matters (anti-DMs). This source is for equal populations of DM and anti-DM, and hence our predicted signals will be upper limits of the predictions. Recently a mechanism of DM-anti-DM oscillations is suggested to reequilibrate the populations at late times [18,19].

[3]We use PYTHIA [20], as implemented in the DarkSUSY [21] or MicrOMEGAs [22] programs, to generate the differential yields (injected particle spectra).

TABLE II. The dark matter density parameters.

Halomodel	α	β	γ	r_s (kpc)
Navarro, Frenk, White	1	3	1	20
Moore	1.5	3	1.5	28
Cored isothermal	2	2	0	5

The charged particles produced by the DM annihilation are predicted to come from the halo near the Sun, not too far from the Sun at least, because they may lose the energy while propagating through the Galactic halo. They are deflected by the Galactic magnetic field, and this property has been described by space diffusion [29]. The charged particles suffer energy losses from synchrotron radiation and inverse Compton scattering. The solar modulation can also induce a certain amount of energy loss. Their energy spectrum at the Earth, therefore, differs from the one produced at the source. The equation that describes the evolution of the energy distribution for the charged particles may be expressed as

$$\begin{aligned}&\frac{\partial}{\partial t}\left(\frac{dn}{dT}\right)_a - \nabla\cdot\left(K(T)\nabla\left(\frac{dn}{dT}\right)_a\right) - \frac{\partial}{\partial T}\left(b(T)\left(\frac{dn}{dT}\right)_a\right)\\ &\quad + \frac{\partial}{\partial z}\left(\mathrm{sign}(z)V_C\left(\frac{dn}{dT}\right)_a\right)\\ &= Q_a(\mathbf{x}, T) - 2h\Gamma_{\rm ann}\delta(z)\left(\frac{dn}{dT}\right)_a,\end{aligned} \tag{4}$$

where dn/dT is the number density of particles per unit volume and energy. The second term accounts for the space diffusion with the energy dependent diffusion constant $K(T) = K_0(T/\mathrm{GeV})$. The energy loss due to synchrotron radiation in the Galactic magnetic field and inverse Compton scattering on CMB photons and on Galactic starlight is described in the third term. The rate of energy loss is $b(T) = T^2/(\mathrm{GeV}\tau_T)$, where $\tau_T = 10^{16}$ s is the energy loss time. The fourth term is the effect of convective wind. The last term accounts for the annihilation of the produced matter(s) in the interstellar medium, H and He atoms, with annihilation rate $\Gamma_{\rm ann}$ in the disk of thickness $2h \simeq 0.2$ kpc, and hence it is provided as a negative source term. The relevant coefficients were parametrized, and the established (transport) parameters were estimated from the analysis of observed isotope ratios in cosmic rays, primarily the boron to carbon (B/C) ratio [30]. Three propagation models have been featured with the established parameters, and these propagation models correspond to minimal, medium, and maximum antiproton fluxes [30,31].

The number density dn/dT is obtained by solving Eq. (4) with the steady state condition $\frac{\partial}{\partial t}(\frac{dn}{dT})_a = 0$ and boundary conditions in a two-zone model [32], where the region of diffusion of cosmic rays is represented by a thick disk of thickness $2L \simeq 5$–20 kpc and radius $R \simeq 20$ kpc, and the thin Galactic disk lies in the middle and has thickness $2h$, radius R. The boundary conditions are such that the number density vanishes at $z = \pm L$ and at $r = R$.

A. The positron channels

The energy spectrum of positrons is obtained by solving the diffusion equation, keeping only contributions of space diffusion and energy losses,

$$-K(E)\nabla^2\left(\frac{dn}{dE}\right)_{e^+} - \frac{\partial}{\partial E}\left(b(E)\left(\frac{dn}{dE}\right)_{e^+}\right) = Q_{e^+}(\mathbf{x}, E), \quad (5)$$

with the relevant parameters listed in Table III. This diffusion equation may be solved by the Green function formalism or the Bessel-transform method, and the solution results in the following form:

$$\left(\frac{dn}{dE}\right)_{e^+} = \frac{1}{b(E)}\int_E^M dE_S Q_{e^+}(\mathbf{x}_\odot, E_S) I_{e^+}(E, E_S), \quad (6)$$

where $\mathbf{x}_\odot$ is the location of the Sun from the Galactic center. The function $I_{e^+}(E, E_S)$ must fully encode the Galactic astrophysics from the input energy E_S to energy $E(\leq E_S)$, and the full expression of this function can be found in Ref. [31].

The positron flux is then given by

$$\begin{aligned}\phi_{e^+} &= B\frac{v_{e^+}}{4\pi}\left(\frac{dn}{dE}\right)_{e^+} \\ &= B\frac{v_{e^+}\langle\sigma v\rangle_f}{16\pi b(E)}\left(\frac{\rho_\odot}{M}\right)^2\int_E^M dE_S\left(\frac{dN^f}{dE}\right)_{e^+} I_{e^+}(E, E_S),\end{aligned} \quad (7)$$

where v_{e^+} is the velocity of the positron.

The enhancement may come from a subhalo structure (dark clumps) and the nonperturbative Sommerfeld effect because one of the force carriers is a photon in this scenario. The enhancement by the Sommerfeld effect can be calculated from the original form [33]. We can split the dipole operator in energy and momentum dependent parts by the familiar Gordon decomposition,

$$\mu\bar{v}(p')\sigma^{\mu\nu}q_\nu u(p) = i\mu\bar{v}(p')(2M\gamma^\mu + (p' - p)^\mu)u(p). \quad (8)$$

In the energy dependent part, we have the same type of coupling with the DM mass dependence as for electric charge. The original Sommerfeld enhancement factor is

$$S = \frac{\pi\alpha_\mu/v}{1 - e^{-\pi\alpha_\mu/v}} \overset{\alpha_\mu \gg v}{\sim} \frac{\pi\alpha_\mu}{v}, \quad (9)$$

where v is the DM velocity ($\sim 10^{-3}$). In the original form, α_μ is the electric fine structure constant, but $\alpha_\mu = 16\pi\mu^2M^2$ in this case. We do not find a series of resonances because the potential is not localized. We have the enhancement $S \simeq 16$ for the DM mass of 100 GeV and magnetic dipole $\mu \simeq 0.1$ TeV^{-1}. According to recent work [34,35], DMs annihilating after recombination may contribute to the CMB anisotropy spectrum, and the enhancement bound could be set up. The CMB bound is $S < (120/f)(M/\text{TeV})$ where the parameter f indicates the average fraction of energy absorbed by the gas and depends on final states. The bound is slightly over 17 for the $e^\pm$ final state, $f \simeq 0.7$. Our enhancement factor lies very near the estimated bound. We can also consider an enhancement from the metastable bound state between DMs, called "WIMPonium." This production process from DMs annihilation is, however, kinematically forbidden, because the estimated kinetic energy ($\sim Mv^2$) with velocity $v \sim 10^{-3}$ is too small to incorporate the binding energy ($\sim M\alpha_\mu^2$).

The strength of the magnetic dipole is, according to Ref. [11], almost constant for the DM mass larger than 100 GeV, and thereby the enhancement increases in the square of the DM mass. Because of this reason, the fluxes, Eq. (7), must have a similar magnitude about the DM masses larger than 100 GeV because the fluxes are not scaled by the DM mass. We notice that the fluxes are scaled by the DM mass in most of the models, and large boost factors have been required for larger DM mass because the fluxes decrease with the square of the DM mass.

The positrons are affected by solar wind and lose energy while transporting in the solar system. This effect leads to a shift in the energy distribution between the interstellar spectrum (IS) and the spectrum at the top of the atmosphere (TOA). This modulation is considered for the predicted fluxes by the relation in force field approximation [36],

$$\phi_{e^+}^{\text{TOA}}(E) = \frac{E^2 - m_{e^+}^2}{(E + |Z|e\Phi)^2 - m_{e^+}^2}\phi_{e^+}^{\text{IS}}(E + |Z|e\Phi), \quad (10)$$

where $|Z|$ is the magnitude of electric charge (1 in this case), e is the electric constant, and Φ is the Fisk potential, namely, solar modulation parameter, which varies between 500 MV and 1.2 GV over the 11-year solar cycle. Since experiments are usually undertaken near solar minimum activity, we choose $\Phi = 600$ MV (the Fisk potential for the PAMELA experiment) for our numerical analysis.

We show in Fig. 1 the predicted positron fractions for the boost factors, $B = 30$, 50, 80, with the computed background[4] from Ref. [37] and several experimental data sets.

TABLE III. Typical diffusion parameters for positrons deduced from a variety of cosmic ray data, which yield the minimum (MIN), median (MED), and maximal (MAX) fluxes.

Model	δ	K_0[kpc^2/Myr]	L(kpc)
MIN	0.55	0.00595	1
MED	0.70	0.0112	4
MAX	0.46	0.0765	15

[4]Secondary positrons from nuclear interactions of cosmic ray nuclei with interstellar gas have been investigated in detail by the authors of Ref. [37]. Recently, it was suggested that the secondary positrons are increased by up to 60% at high energies above 100 GeV [38], based on analysis of the spectral hardening in the cosmic ray proton and helium fluxes reported by the ATIC2 [39] and CREAM [40] balloon experiments.

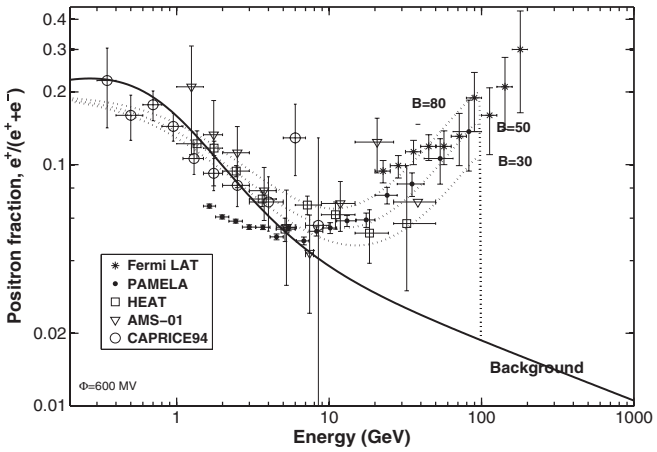

FIG. 1. Positron fraction from the annihilation of the fermionic dark matter particle. The boost factors have been chosen to provide qualitatively good fits to the data with dark matter mass 100 GeV. Shown are the background (solid line) and the experimental data sets of the PAMELA [41], HEAT [42], AMS-01 [43], Fermi LAT [44], and CAPRICES94 [58] experiments.

The predicted fractions have almost no difference[5] in the halo profiles or the diffusion models. The predicted fractions exhibit a rather sharp distribution at $E_{e^+} \simeq M$, since our candidate can directly annihilate into an electron and positron pair. The PAMELA experiment [41] has shown a steep rise in the 10–100 GeV range in their measurements and confirmed the results of the HEAT [42] and AMS-01 [43] experiments. Recently, the steep rise has been extended to 200 GeV with three more data points over 100 GeV at the Fermi LAT [44]. The predicted signals with the boost factor 30–80 nicely fit measurements of the PAMELA experiment for the DM mass of around 100 GeV. An enhancement of about a factor of 16 comes from the Sommerfeld effect, and for the rest an enhancement factor of 2–5 is expected to come from a subhalo structure (dark clumps). The existence of subhalos is a generic prediction of the ΛCDM scenario of structure formation in the Universe, and high resolution simulations [45] show that the large scale structures form by continuous merging of smaller hallos that could be in the form of subhalos. The contribution of subhalos to the flux could be constrained from analysis of CMB data that do not rely on uncertain assumptions of the DM distribution [46]. The subhalo boost factor has been predicted to be 10 [46] at most. Extracting the accurate formalism of this boost factor is out of the scope of this paper. Our subhalo boost factors must be in a reasonable range.

We also have the difference between predictions and experimental measurements or background at low energies ($\leq$10 GeV). It has been noticed that the solar modulation effect we consider has no charge-sign dependence and has to be modified. This must be left for a future study.

[5]If we only consider the fractions or fluxes of signals excluding the background, there are sizable differences at the low energies less than 10 GeV, especially in diffusion models.

TABLE IV. Typical diffusion parameters for antiprotons deduced from a variety of cosmic ray data that yield the minimum, median, and maximal fluxes.

Model	δ	K_0[kpc^2/Myr]	V_C(km/s)	L(kpc)
MIN	0.85	0.0016	13.5	1
MED	0.70	0.0112	12	4
MAX	0.46	0.0765	5	15

B. The antiproton channels

The propagation of antiprotons is dominated by diffusion and the effect of the Galactic wind. The energy spectrum of antiprotons is obtained by solving the following diffusion equation:

$$\frac{\partial}{\partial z}\left(\mathrm{sign(z)V_C}\left(\frac{\mathrm{dn}}{\mathrm{dT}}\right)_{\bar{\mathrm{p}}}\right) - \nabla\cdot\left(K(T)\nabla\left(\frac{dn}{dT}\right)_{\bar{p}}\right) = Q_a(\mathbf{x},T) - 2h\Gamma_{\mathrm{ann}}\delta(z)\left(\frac{dn}{dT}\right)_{\bar{p}}, \tag{11}$$

with the relevant parameters listed in Table IV. An important difference with the positron case is that energy loss of antiprotons is negligible, because antiprotons are more massive and hence it is absent in the diffusion equation (11).

The antiproton flux is then given by

$$\phi_{\bar{p}} = B\frac{v_{\bar{p}}}{4\pi}\left(\frac{dn}{dT}\right)_{\bar{p}} = B\frac{v_{\bar{p}}\langle\sigma v\rangle_f}{16\pi}\left(\frac{dN^f}{dT}\right)_{\bar{p}}\left(\frac{\rho_\odot}{M}\right)^2 I_{\bar{p}}(T), \tag{12}$$

where the function $I_{\bar{p}}(T)$ encodes all the astrophysics, and the full expression can be found in Refs. [47,48].

Figure 2 shows the predicted ratios of antiproton over proton with the computed background [49] and several experimental measurements. As in the case of the positrons, the predictions have almost no difference in the halo profiles, but they are sensitive to the propagation models. The predictions in the MIN propagation model are selected, and they may be within the invisible range for current detectors. However, this scenario is most likely ruled out for other propagation models,[6] MED and MAX, because the predicted fluxes in MED or MAX propagation models are about 10 or 100 times larger than the ones in the MIN propagation model.

[6]To be strict, the MED propagation model can also be viable because of the uncertainty of the transport parameters. The parameters are established by the best fit of cosmic ray B/C data [30]. However, the assigned values of transport parameters may differ by 1 order of magnitude.

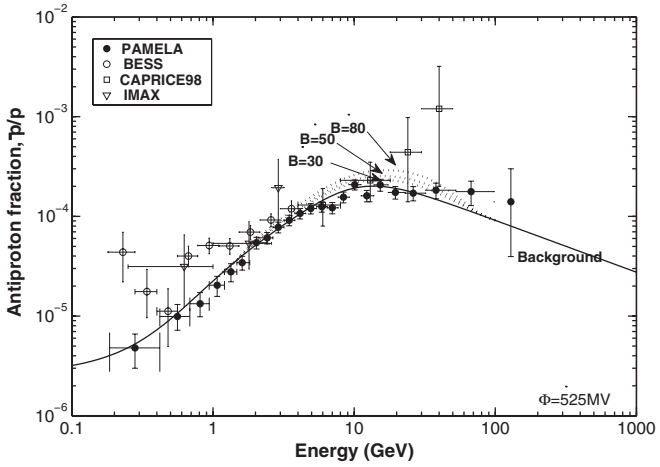

FIG. 2. Antiproton over proton ratio as a function of kinetic energy. Shown are the background (solid line) and the experimental data sets of the PAMELA [59], BESS [60], CAPRICE98 [61], and IMAX [62] experiments.

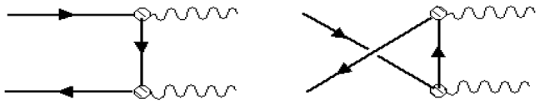

FIG. 3. Feynman diagrams for annihilation of dark matter to one photon or two photons. The hatched circles indicate the dipole couplings.

C. The gamma-ray channels

The production of gamma rays has been considered to be a very important channel to search for the DM signals, since they travel in straight lines and can travel greater distances without energy loss. For these reasons, they contain spectral and directional information that can be well measured. The gamma-ray flux from the DM annihilations at a given photon energy from a direction that forms an angle ψ between the direction of the Galactic center and that of observation is accounted for by the line-of-sight (los) integration method,

$$\phi_\gamma = B\frac{\langle\sigma v\rangle_f}{16\pi M^2}\left(\frac{dN^f}{dE}\right)_\gamma \int_{\rm los} \rho^2(r(s,\psi))ds, \qquad (13)$$

where $r = \sqrt{r_\odot^2 + s^2 - 2r_\odot s\cos\psi}$ is the Galactocentric distance. In terms of the galactic latitude b and longitude l, one has $\cos\psi = \cos b\cos l$. The coordinate s parametrizes the distance from the Sun along the los.

This form can be reduced to

$$\phi_\gamma \simeq 8.31\times10^{-11}\ (\mathrm{cm}^2\cdot\mathrm{sr}\cdot\mathrm{s})^{-1}\cdot\frac{B\langle\sigma v\rangle_f}{10^{-26}\ \mathrm{cm}^3\,\mathrm{s}^{-1}} \times\left(\frac{100\ \mathrm{GeV}}{M}\right)^2\left(\frac{dN^f}{dE}\right)_\gamma\cdot\bar{J}_{\Delta\Omega}, \qquad (14)$$

where $\bar{J}_{\Delta\Omega}$ is a dimensionless los integral averaged over the solid angle $\Delta\Omega$ and is defined by

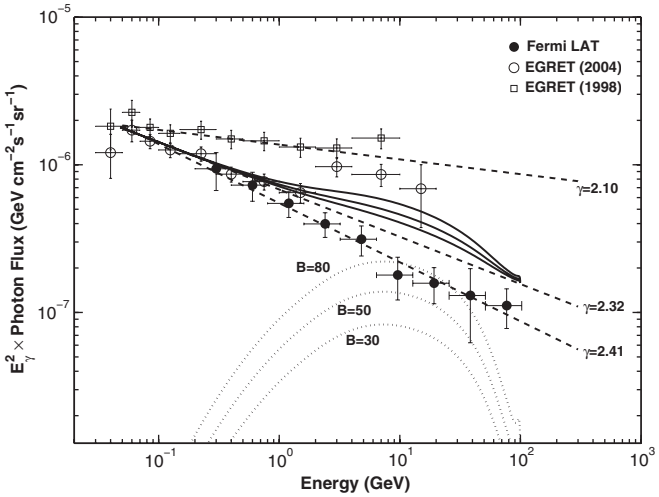

FIG. 4. The gamma-ray spectrum from Galactic halo for the dark matter mass of 100 GeV and the region, $0^\circ \le \ell \le 360^\circ$, $|b| \ge 10^\circ$. Shown are the experimental data sets from the Fermi LAT and EGRET with their fitted spectral indices.

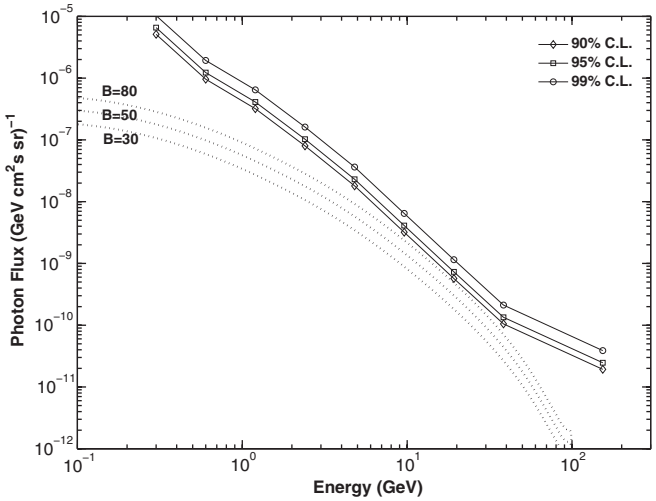

FIG. 5. The gamma-ray flux from Galactic halo for the dark matter mass of 100 GeV and the target region $0^\circ \le \ell \le 360^\circ$, $|b| \ge 10^\circ$ with 90, 95, and 99 C.L. experimental limits of the Fermi LAT.

$$\bar{J}_{\Delta\Omega} = \frac{1}{\Delta\Omega}\int J(\psi)d\Omega, \qquad (15)$$

with

$$J(\psi) = \int \frac{\rho^2(r)}{\rho_\odot^2}\frac{ds}{r_\odot}. \qquad (16)$$

In addition to the continuum emission, the direct DM annihilations produce $\gamma\gamma$ and γZ final states[7] in this

[7]The production of the single γ or Z final state is prohibited, because in this process it is impossible to conserve energy and momentum together.

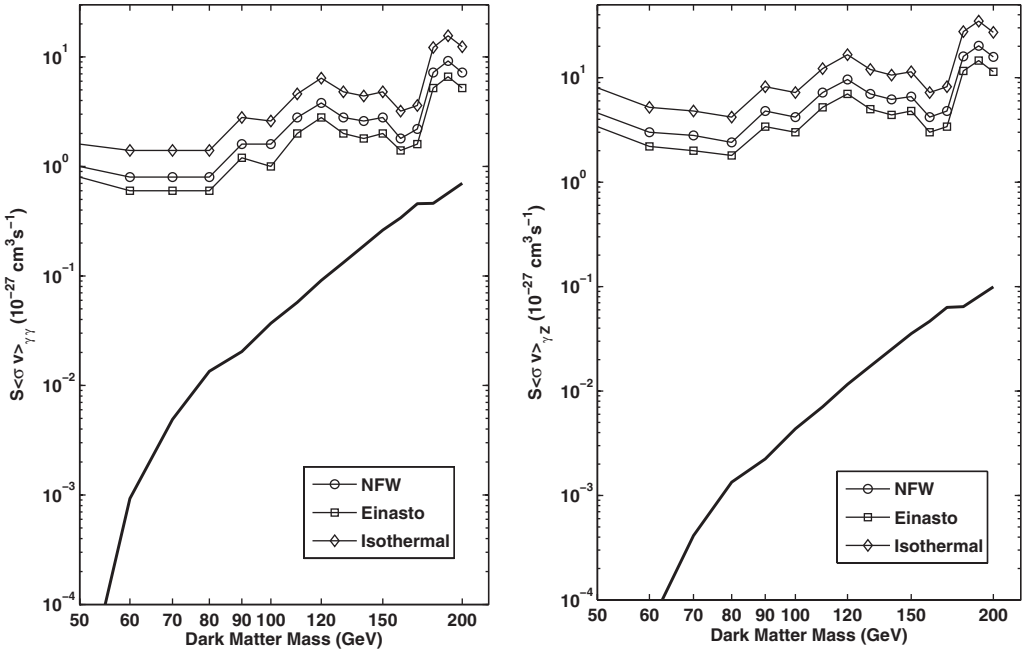

FIG. 6. Annihilation rates with Sommerfeld enhancement factor S for dark matter annihilation to $\gamma\gamma$ or γZ. Shown are the 95% C.L. upper limits of the Fermi LAT for the region $|b| \geq 10^\circ$ plus a $20^\circ \times 20^\circ$ square centered at the Galactic center.

scenario, in which Feynman diagrams are shown in Fig. 3. Such processes would yield the very distinctive feature of monoenergetic gamma-ray lines (monochromatic photons) with an energy $E_\gamma = M$ or $M(1 - m_Z^2/(2M)^2)$. The full annihilation rates for the production of $\gamma\gamma$ are $\langle\sigma v\rangle_{\gamma\gamma} = \mu^4 M^2/2\pi$ and $\langle\sigma v\rangle_{\gamma Z} = \mu^4 M^2 \beta_Z^2 \tan^2\theta_W/4\pi$ for γZ. The contributions for $\gamma\gamma$ and γZ final states are suppressed by the magnetic dipole μ^4, and the γZ final state has an additional suppression with Weinberg angle $\tan^2\theta_W$.

We restrict our analysis to the possible signals from the Galactic halo as in the case of the positrons for a complementarity, and the same boost factors[8] $B = 30, 50, 80$ are selected. We compare our predictions to experimental observations in two stringent cases. One is a process that may contribute to the extragalactic gamma-ray background (EGB). The other is, in the case that astrophysical sources account for the EGB in the entire energy range, a process that satisfies the experimental exclusion limit of the Fermi LAT [50].

Figure 4 shows the predicted gamma-ray spectra as a function of photon energy in the region $0^\circ \leq \ell \leq 360^\circ$, $|b| \geq 10^\circ$. The spectra are superpositions of the continuum and monoenergetic gamma rays at the DM mass of 100 GeV. The spectra have almost no difference in the halo profiles. The EGB from the Fermi LAT [50] is given by

$$E_\gamma^2 \phi_\gamma \simeq 5.5 \times 10^{-7} \left(\frac{E}{1\ \text{GeV}}\right)^{-0.41} (\text{cm}^2 \cdot \text{sr} \cdot \text{s})^{-1}\ \text{GeV}. \quad (17)$$

The same type of background from the analysis of the EGRET measurements is also described [51] from the first analysis [52]. The predicted spectra are not exceeding the EGB, and we might have a signature if it can be disentangled from astrophysical ones. In addition, we check if our prediction can account for the EGRET anomaly,[9] which is not confirmed at the Fermi LAT. Our predictions are too soft to explain the observation of the EGB, and more enhancement would be needed.

The predicted fluxes have to be within the uncertainty of Fermi LAT data, in the case that the EGB is accounted for by astrophysical sources in the entire energy range. Figure 5 shows the predicted fluxes with 90, 95, and 99% C.L. experimental limits of the Fermi LAT, which are estimated from the data table in Ref. [50]. The predictions are smaller than the exclusion limits and so satisfy the current experimental constraint.

The Galactic center or the region close to it must be the most complex region in the Galaxy due to many possible sources and the difficulty to model the diffuse emission. Hence, it may be very difficult to disentangle possible DM annihilation signals from the background fluxes. The monochromatic gamma-ray lines appearing from DM

[8]It has been predicted that the possible enhancement from the subhalo has an angular and/or energy dependence on the cosmic rays. The enhancement can be different in each channel, but there are still no clear experimental evidences for dark clumps. We select the same boost factors, $B = 30$–80, for a reference. The main idea of the enhancement from a subhalo structure comes from $\langle\rho^2\rangle \geq \langle\rho\rangle^2$.

[9]Although this anomaly is likely caused by a systematic error of the effective detector sensitivity calibration [53], we include this anomaly in our analysis for a possible signal in case.

annihilations could provide smoking-gun signatures for these regions, because the line signals mostly cannot be mistaken for an astrophysical source.

Figure 6 shows the predicted annihilation rate for $\gamma\gamma$ and γZ final states as a function of the DM mass. The Sommerfeld effect is included but not the subhalo structure. The strength of the DM magnetic dipole is chosen to satisfy the relic density from Ref. [11]. The curves given for the NFW, Einasto, and isothermal DM distributions are 95% C.L. upper limits of Fermi LAT [54] for the region $|b| \geq 10^\circ$ plus a $20^\circ \times 20^\circ$ square centered at the Galactic center. The predicted annihilation rates are approximately 4.0×10^{-29} cm^3/s at $E_\gamma \simeq 100$ GeV for the $\gamma\gamma$ final state and 4.0×10^{-30} cm^3/s for the γZ final state at $E_\gamma \simeq 80$ GeV. Otherwise, the estimated upper limits at the Fermi LAT are 10^{-27}–10^{-26} cm^3/s for both final states, depending on the DM mass and the halo profiles. The predictions are 2 or 3 orders smaller than the experimental upper limits. However, our predictions can be enhanced if dense DM clumps are considered in regions close to the Galactic center. Recently, the authors of Refs. [55,56] pointed out the gamma-ray excess, 1–3×10^{-27} cm^3/s, around 130 GeV in the spectrum based on these measurements with 4.5 or 6σ statistical significance. Our predictions with the subhalo boost factor of about 100 can account for the gamma-ray excess.

One of the reasons we mostly get the low predictions for sharp peaks is due to the relatively poor energy resolution. The current energy resolution of the Fermi LAT is 11–13% [54] in the full width at half maximum. The energy resolution could be as good as 1.5–2% for a planned experiment, AMS-02 [57], in which the upper limits of the annihilation rate will be 10^{-30}–10^{-29} cm^3/s. Our predicted signals are in the potential probe at the AMS-02.

III. CONCLUSION

We considered cosmic ray signals in the positron, antiproton, and photon channels of dipole-interacting DM annihilation. The predicted signals in the positron channel could nicely account for the excess of positron fraction from Fermi LAT, PAMELA, HEAT, and AMS-01 experiments for the DM mass larger than 100 GeV with a boost factor of 30–80. An enhancement of about a factor of 16 could come from the Sommerfeld nonperturbative effect and the rest an enhancement factor of 2–5 from a subhalo structure (dark clumps). The predicted signals have almost no dependence on the DM mass because of the Sommerfeld effect. No excess of antiproton over proton ratio at the experiments also gives a severe restriction for our scenario. This scenario may be viable for a MIN Galactic propagation model but likely ruled out for other propagation models, MED and MAX. The predicted signals from the Galactic halo in the region $0^\circ \leq \ell \leq 360^\circ$, $|b| \geq 10^\circ$, and signals as the monoenergetic gamma-ray lines (monochromatic photons) for the region ($|b| \geq 10^\circ$ plus a $20^\circ \times 20^\circ$ square centered at the Galactic center) close to the Galactic center were also considered. The predicted signals from the Galactic halo must satisfy the current experimental constraint, and the signals for the region near the Galactic center as monoenergetic lines must be smaller than the experimental exclusion limits of the Fermi LAT. The gamma-ray excess 1–3×10^{-27} cm^3/s around 130 GeV, pointed out by the authors of Refs. [55,56], could be accounted for in this scenario, with the subhalo boost factor of about 100. Our predicted signals as monoenergetic lines for the region near the Galactic center are also in the potential probe at the planned experiment, AMS-02, with the better experimental method.

ACKNOWLEDGMENTS

The work was supported by a National Research Foundation of Korea (NRF) grant funded by the Korea Government of the Ministry of Education, Science and Technology (MEST) (Grant No. 2011-0017430) and (Grant No. 2011-0020333).

[1] E. Komatsu *et al.* (WMAP Collaboration), Astrophys. J. Suppl. Ser. **192**, 18 (2011).
[2] A. Borriello and P. Salucci, Mon. Not. R. Astron. Soc. **323**, 285 (2001).
[3] H. Hoekstra, H. Yee, and M. Gladders, New Astron. Rev. **46**, 767 (2002).
[4] C. Alcock *et al.* (MACHO Collaboration), Astrophys. J. **542**, 281 (2000).
[5] R. Bernabei *et al.* (DAMA Collaboration), Riv. Nuovo Cimento Soc. Ital. Fis. **26**, 1 (2003); Int. J. Mod. Phys. D **13**, 2127 (2004).
[6] R. Bernabei *et al.* (DAMA Collaboration), Eur. Phys. J. C **56**, 333 (2008).
[7] B. Feldstein, P. W. Graham, and S. Rajendran, Phys. Rev. D **82**, 075019 (2010).
[8] T. Lin and D. P. Finkbeiner, Phys. Rev. D **83**, 083510 (2011); S. Chang, N. Weiner, and I. Yavin, Phys. Rev. D **82**, 125011 (2010); J. Shu, P. Yin, and S. Zhu, Phys. Rev. D **81**, 123519 (2010); S. Chang, G. D. Kribs, D. Tucker-Smith, and N. Weiner, Phys. Rev. D **79**, 043513 (2009).
[9] H. An, S. Chen, R. M. Mohapatra, S. Nussinov, and Y. Zhang, Phys. Rev. D **82**, 023533 (2010); M. Pospelov and A. Ritz, Phys. Lett. B **671**, 391 (2009).
[10] B. Feldstein, A. L. Fitzpatrick, E. Katz, and B. Tweedie, J. Cosmol. Astropart. Phys. 03 (2010) 029; S. Chang,

A. Pierce, and N. Weiner, J. Cosmol. Astropart. Phys. 01 (**2010**) 006.
[11] J. Ho Heo, Phys. Lett. B **693**, 255 (2010); **702**, 205 (2011).
[12] M. Pospelov and T. Veldhuis, Phys. Lett. B **480**, 181 (2000).
[13] K. Sigurdson, M. Doran, A. Kurylov, R. R. Caldwell, and M. Kamionkowski, Phys. Rev. D **70**, 083501 (2004); **73**, 089903(E) (2006).
[14] V. Barger, W.-Y. Keung, and D. Marfatia, Phys. Lett. B **696**, 74 (2011).
[15] W. S. Cho, J.-H. Huh, I.-W. Kim, J. E. Kim, and B. Kyae, Phys. Lett. B **687**, 6 (2010); **694**, 496(E) (2011).
[16] T. Banks, J.-F. Fortin, and S. Thomas, arXiv:1007.5515.
[17] E. D. Nobile, C. Kouvaris, P. Panci, F. Sannino, and J. Virkajärvi, J. Cosmol. Astropart. Phys. 08 (2012) 010.
[18] S. Tulin, H.-B. Yu, and K. M. Zurek, J. Cosmol. Astropart. Phys. 05 (2012) 013.
[19] M. Cirelli, P. Panci, G. Servant, and G. Zaharijas, J. Cosmol. Astropart. Phys. 03 (2012) 015.
[20] T. Sjostrand, S. Mrenna, and P. Skands, Comput. Phys. Commun. **178**, 852 (2008).
[21] P. Gondolo, J. Edsjo, P. Ullio, L. Bergstrom, M. Schelke, and E. A. Baltz, J. Cosmol. Astropart. Phys. 07 (2004) 008.
[22] G. Belanger, F. Boudjema, P. Brun, A. Pukhov, S. Rosier-Lees, P. Salati, and A. Semenov, Comput. Phys. Commun. **182**, 842 (2011).
[23] J. F. Navarro, C. S. Frenk, and S. D. M. White, Astrophys. J. **490**, 493 (1997).
[24] B. Moore, F. Governato, T. Quinn, J. Stadel, and G. Lake, Astrophys. J. **499**, L5 (1998); J. Diemand, B. Moore, and J. Stadel, Mon. Not. R. Astron. Soc. **353**, 624 (2004).
[25] J. N. Bahcall and R. M. Soneira, Astrophys. J. Suppl. Ser. **44**, 73 (1980).
[26] J. Einasto, Trudy Inst. Astroz. Alma-Ata **51**, 87 (1965).
[27] J. F. Navarro *et al.*, arXiv:0810.1522.
[28] R. Catena and P. Ullio, J. Cosmol. Astropart. Phys. 08 (2010) 004.
[29] F. Casse, M. Lemoine, and G. Pelletier, Phys. Rev. D **65**, 023002 (2001).
[30] F. Donato, N. Fornengo, D. Maurin, P. Salati, and R. Taillet, Phys. Rev. D **69**, 063501 (2004); D. Maurin, F. Donato, R. Taillet, and P. Salaati, Astrophys. J. **555**, 585 (2001).
[31] T. Deliahaye, R. Lineros, F. Donato, N. Fornengo, and P. Salati, Phys. Rev. D **77**, 063527 (2008).
[32] F. Donato, D. Maurin, P. Salati, A. Barrau, G. Boudoul, and R. Taillet, Astrophys. J. **563**, 172 (2001).
[33] A. Sommerfeld, Ann. Phys. (Berlin) **403**, 257 (1931); J. Hisano, S. Matsumoto, and M. M. Nojiri, Phys. Rev. Lett. **92**, 031303 (2004).
[34] T. R. Slatyer, N. Padmanabhan, and D. P. Finkbeiner, Phys. Rev. D **80**, 043526 (2009).
[35] S. Galli, F. Iocco, G. Bertone, and A. Melchiorri, Phys. Rev. D **80**, 023505 (2009).
[36] L. J. Gleeson and W. I. Axford, Astropart. Phys. **154**, 1011 (1968); **149**, L115 (1967).
[37] I. V. Moskalenko and A. W. Strong, Astrophys. J. **493**, 694 (1998); E. A. Baltz and J. Edsjo, Phys. Rev. D **59**, 023511 (1998).
[38] J. Lavalle, Mon. Not. R. Astron. Soc. **414**, 985 (2011).
[39] A. D. Panov *et al.*, Bull. Russ. Acad. Sci. Phys. **73**, 564 (2009).
[40] H. S. Ahn *et al.*, Astrophys. J. **714**, L89 (2010).
[41] O. Adriani *et al.* (PAMELA Collaboration), Nature (London) **458**, 607 (2009); O. Adriani, G. C. Barbarino, G. A. Bazilevskaya, R. Bellotti, M. Boezio, E. A. Bogomolov, L. Bonechi, M. Bongi, V. Bonvicini, and S. BorisovAstropart. Phys. **34**, 1 (2010).
[42] S. W. Barwick *et al.* (HEAT Collaboration), Astrophys. J. **482**, L191 (1997).
[43] M. Aguilar *et al.* (AMS-01 Collaboration), Phys. Lett. B **646**, 145 (2007).
[44] M. Ackermann *et al.* (Fermi LAT Collaboration), Phys. Rev. Lett. **108**, 011103 (2012).
[45] J. Diemand, M. Kuhlen, P. Madau, M. Zemp, B. Moore, D. Potter, and J. Stadel, Nature (London) **454**, 735 (2008); J. Diemand, M. Kuhlen, and P. Madau, Astrophys. J. **657**, 262 (2007).
[46] L. Pieri, J. Lavalle, G. Bertone, and E. Branchini, Phys. Rev. D **83**, 023518 (2011).
[47] P. Chardonnet, G. Mignola, P. Salati, and R. Taillet, Phys. Lett. B **384**, 161 (1996).
[48] L. Bergstrom, J. Edsjo, and P. Ullio, Astrophys. J. **526**, 215 (1999).
[49] A. M. Lionetto, A. Morselli, and V. Zdravkovic, J. Cosmol. Astropart. Phys. 09 (2005) 010; T. Bringmann and P. Salati, Phys. Rev. D **75**, 083006 (2007).
[50] A. A. Abdo *et al.* (Fermi LAT Collaboration), Phys. Rev. Lett. **104**, 101101 (2010).
[51] A. W. Strong, I. V. Moskalenko, and O. Reimet, Astrophys. J. **613**, 956 (2004); **613**, 962 (2004).
[52] P. Sreekumar *et al.* (EGRET Collaboration), Astrophys. J. **494**, 523 (1998).
[53] F. W. Stecker, S. D. Hunter, and D. A. Kniffen, Astropart. Phys. **29**, 25 (2008).
[54] M. Ackermann *et al.* (Fermi LAT Collaboration), Phys. Rev. D **86**, 022002 (2012): A. A. Abdo *et al.* (Fermi LAT Collaboration), Phys. Rev. Lett. **104**, 091302 (2010).
[55] C. Weniger, J. Cosmol. Astropart. Phys. 08 (2012) 007.
[56] E. Tempel, A. Hektor, and M. Raidal, J. Cosmol. Astropart. Phys. 09 (2012) 032; 11 (2012) A01.
[57] A. Kounine, arXiv:astro-ph/1009.5349; http://ams.cern.ch.
[58] M. Boezio *et al.* (WIZARD Collaboration), Astrophys. J. **532**, 653 (2000).
[59] O. Adriani *et al.* (PAMELA Collaboration), Phys. Rev. Lett. **105**, 121101 (2010).
[60] Y. Asaoka *et al.*, Phys. Rev. Lett. **88**, 051101 (2002).
[61] M. Boezio *et al.* (WIZARD/CAPRICE Collaboration), Astrophys. J. **561**, 787 (2001).
[62] J. W. Mitchell *et al.*, Phys. Rev. Lett. **76**, 3057 (1996).